Resonant electron capture in $Al_xGa_{1-x}As$/AlAs/GaAs quantum wells

A. Fujiwara,* Y. Takahashi,† S. Fukatsu,‡ and Y. Shiraki
Research Center for Advanced Science and Technology (RCAST), The University of Tokyo, 4-6-1 Komaba, Meguro-ku, Tokyo 153, Japan

R. Ito
Department of Applied Physics, Faculty of Engineering, The University of Tokyo, 7-3-1 Hongo, Bunkyo-ku, Tokyo 153, Japan
(Received 13 July 1994)

Resonant electron capture in $Al_xGa_{1-x}As$/AlAs/GaAs quantum-well structures is systematically investigated by means of both continuous-wave and time-resolved photoluminescence. The capture efficiency and the capture time of barrier electrons into quantum wells both exhibit a clear oscillation as a function of well width. The enhanced capture efficiency in the oscillation is ascribed to the resonant electron capture. It is also revealed that the resonant effect is drastically enhanced by the insertion of AlAs tunnel barriers at both heterointerfaces and controlled by their widths. The resonant well width can be well described within the framework of the effective-mass approximation. An oscillating capture time due to the resonant electron capture is observed between 175–480 and 43–270 psec for 20- and 10-Å tunnel barriers, respectively. Investigation of the temporal profile of the quantum-well luminescence suggests ambipolar capture of the carriers due to the charge buildup effect.

I. INTRODUCTION

The capture of electrons and holes into a quantum well (QW) has been attracting considerable interest from the viewpoint of device application such as semiconductor QW lasers as well as the underlying physical mechanism. The capture process, in which the carrier in the barrier relaxes down to the bound state in QW's should be treated rigorously in terms of quantum mechanics since the well width (L_z) is small enough for the electron to behave as a wave. Initial studies of carrier capture in QW's, however, have been based on the classical diffusion model,[1–3] where the diffusing carrier in the barrier is captured into the well when it crosses the well and is scattered by LO phonons. From this viewpoint it was reported that the capture efficiency is decreased when the well width is smaller than the inelastic mean free path of electrons. A theoretical study of the quantum-mechanical carrier capture in QW's was reported by Kozyrev and Shik[4] and later by Brum and Bastard.[5] It was predicted in their calculation that the carrier capture time shows an oscillatory behavior as a function of L_z, and that the carrier capture rate is enhanced when L_z is such that the highest bound states in the QW lines up with the barrier band edge. In this situation, the wave function of the carrier in the barrier band edge is likely to be concentrated in the well, and its increased overlap with the wave function of bound states in QW's leads to an enhanced capture rate. Hereafter, we refer to this resonance effect as resonant carrier capture. From the viewpoint of the wave packet, resonant carrier capture can be attributed to the increased residence time of the incoming barrier carrier in QW virtual bound states.[6,7] Brum and Bastard[5] also predicted another class of quantum-mechanical resonance due to the enhancement of electron–LO-phonon interaction. This type of resonance occurs when the energy of a bound state is below the energy of the barrier band edge by the energy of a LO phonon. In such a band configuration, the initial barrier band edge state can couple with the bound state by the emission of a LO phonon with in-plane wave vector being reduced to zero. Since the scattering rate by the LO phonon falls off with phonon wave vector q according to q^{-2}, the capture rate is enhanced. Babiker *et al.*[8] predicted another type of resonance for the carrier capture rate by considering two-dimensional phonons. The resonance arises when there is confinement of an additional phonon mode in the well.

Experimentally, however, the resonant carrier capture was by no means easy to observe. In a previous study of carrier capture time by time-resolved photoluminescence (PL),[9–14] it was evaluated from the decay time of the barrier PL and/or the rise time of the QW PL. One reason for the difficulty in observing the resonant carrier capture is that the carrier capture time is likely to be of the same order of magnitude or faster than the relaxation time of other processes. In fact, there are several relaxation processes (relaxation times) in carrier dynamics in conventional PL measurements: (i) photogeneration of carriers with an excess energy in the barrier; (ii) relaxation down to the barrier band edge ($\sim$psec), (iii) (a) radiative recombination in the barrier band edge ($\sim$nsec) and (b) capture into QW's (relaxation to the bound states in QW's); (iv) intersubband and/or intrasubband relaxation down to the ground bound state (subpicoseconds[15,16]); (v) exciton formation (in-plane wave vector $K\neq 0$);[17] (vi) relaxation within the exciton branch to $K=0$,[17] and (vii) exciton recombination. Experimentally, capture times of <20 (Ref. 10) and 2–3 psec (Ref. 13) were reported in $Al_xGa_{1-x}As$/GaAs single QW's (SQW's). A capture time of 4 psec (Ref. 11) and an electron capture time of

<1 psec (Ref. 9) were shown in $In_xGa_{1-x}As/InP$ QW structures. The oscillations in such a fast time due to the resonant carrier capture might be smoothed out by other, slower processes. Another problem for the observation of the resonant carrier capture is whether the resonant effect is sufficiently large or not. The resonant carrier capture is a quantum-mechanical interference effect of the incoming electron wave and therefore is well described by an analogy to the optics. In this analogy, the QW structure can be regarded as a Fabry-Perot resonator. The heterointerface of the QW corresponds to the optical mirror in the Fabry-Perot resonator. In such a resonator, the magnitude of the resonant effect is dominated by the quantum-mechanical reflectivity at the QW interface which is determined by the height of the potential step at the interface.

We observed the resonant electron capture in the study of the carrier capture efficiency by continuous-wave (cw) PL measurements in $Al_xGa_{1-x}As/GaAs$ QW structures which is specially designed to overcome these problems.[18,19] The structure contains AlAs tunnel barriers at QW interfaces. The insertion of tunnel barriers at QW interfaces increases the quantum-mechanical reflectivity at QW interfaces and enhances the resonant effect. It also reduces the carrier capture rate significantly and prevents the resonant carrier capture from being obscured by the other relaxation processes. We also proposed that the resonant electron capture in QW's with tunnel barriers can be well controlled by changing the width of the tunnel barrier.[20] Recently, Morris *et al.*[21] took advantage of this type of structure and showed that the electron-capture time depends on L_z.

The pump-probe technique has also been successfully utilized in investigating the resonant electron capture. Barros *et al.*[22] measured the carrier capture time by the pump and probe differential transmission measurements and an oscillating capture time between 650 (fsec) and -1.8 psec was obtained. The photon energy of the pump and probe light was in resonance with the band edge of the barrier, in contrast to previous PL measurements where the photogenerated carriers had a large excess energy. This eliminates relaxation processes that would otherwise obscure the capture process. The transmission of the probe light reflects the population decay of electrons in the barrier band edge. Blom *et al.*[23] measured the capture time by pump-probe correlation measurements of the population decay of electrons in the barrier and obtained a capture time oscillating between 3 and 20 psec. However, these recent reports have not systematically examined the L_z dependence. A systematic investigation of the L_z dependence is necessary to determine the capture time due to the resonant electron capture because the resonant condition is rather severe on L_z.

It should be noted that there have been several experimental reports indicating that the electron-capture efficiency is reduced under resonant conditions. Mishima and co-workers[24,25] reported the L_z dependence of the PL efficiency in $Al_xGa_{1-x}As/GaAs$ SQW's. They showed that excitation intensity dependence of the PL intensity varied periodically with L_z, and that the PL efficiency was reduced under the resonant condition for electrons. We also reported that L_z dependence of PL excitation spectra in $Al_xGa_{1-x}As/GaAs$ SQW's showed the reduced capture efficiency under the resonant condition.[26] These results seem to contradict the theoretical prediction of the enhanced capture efficiency due to the resonant electron capture. We have revealed that this discrepancy results from the optical quality of the sample. That is, the anomalous reduction of the PL efficiency under the resonant condition can be attributed to the enhancement of nonradiative recombination under resonant conditions. Details will be discussed elsewhere.[27]

In this paper, we present an experimental study of the resonant electron capture in $Al_xGa_{1-x}As/GaAs$ QW structures, and discuss its physical mechanism. A systematic investigation of the dependence of the carrier capture efficiency and the carrier capture time on L_z and tunnel barrier width (L_{tb}) has been carried out. In Sec. II, a general description of the resonant carrier capture will be given, and its analogy to optical Fabry-Perot resonators will be demonstrated. In Sec. IV, an experimental study of the resonant electron capture will be demonstrated based on the measurement of the carrier capture efficiency in $Al_xGa_{1-x}As/AlAs/GaAs$ QW's using continuous wave (cw) PL. The dependence of the resonant electron capture on tunnel-barrier width and temperature will be also shown and discussed. In Sec. V, a time-resolved PL study of the resonant electron capture will be described. The resonant electron-capture time is obtained from the decay time of the barrier PL. The conclusion will be given in Sec. VI.

II. OPTICAL ANALOGY OF THE RESONANT CARRIER CAPTURE

A. General description of the resonant carrier capture

In the capture process, the initial state is the continuum state at the three-dimensional barrier band edge, and the final state is the bound state of the two-dimensional QW. The capture rate is dominated by the overlap of wave functions between these states. When we choose the proper potential depth (V_e) and well width (L_z), the wave function of the barrier electron in the continuum edge resonantly enters the well region. The resultant increase of its overlap with the wave function of the bound state leads to the enhancement of the capture rate. The phenomenon can be described as the resonant scattering of the barrier electron by the QW potential. The resonant condition is such that the transmissivity of electrons through the QW potential is unity. It is given by

$$k_w L_z=(n-1)\pi \quad (n=1,2,3,\ldots)\,, \tag{1}$$

where k_w is the z-direction wave number of the incoming electron in the well. k_w is determined by the potential depth V_e and the kinetic energy of the incoming electron E as $k_w=\sqrt{2m_w(E+V_e)}/\hbar$, where m_w is the effective mass of the electron in the well. The barrier state under the resonant condition is referred to as a virtual bound state of QW's in analogy with virtual (metastable) states in nuclear physics.[28,29] When the wave packet of the barrier electron encounters the QW, the electron is scattered

by the QW. Under the resonant condition, the residence time of the electron in the well is increased. Such a temporary state, which can be defined within a finite lifetime, is called the "virtual" bound state in QW's. The virtual bound state has a certain energy width which is given by the inverse of the lifetime according to the uncertainty principle. From the viewpoint of the virtual bound state, the resonant carrier capture can be attributed to the enhanced capture rate due to the increased residence time of the incoming electron in the well.

B. Analogy to optical resonators

The resonant carrier capture is a quantum-mechanical interference effect of the barrier electron. In analogy to optics, the QW can be regarded as a Fabry-Perot resonator of the barrier electron wave. The QW interface then corresponds to an optical mirror in a Fabry-Perot resonator. In such a resonator, the ratio of the square amplitude of the wave function for the incident electron in the well (as averaged in the well) over that in the barrier is expressed as

$$\left|\frac{\psi_w}{\psi_b}\right|^2=\frac{t_{wb}^2\left[1+R+2\sqrt{R}\,\frac{\sin 2k_wL_z}{2k_wL_z}\right]}{(1-R)^2+4R\sin^2k_wL_z}, \tag{2}$$

where R represents the quantum-mechanical reflectivity of the interface mirror, and t_{wb} represents the quantum-mechanical transmission coefficient through the interface mirror into the well. R and t_{wb} are given as

$$R=\left[\frac{v_w-v_b}{v_w+v_b}\right]^2, \tag{3}$$

$$t_{wb}=\frac{2v_b}{v_w+v_b}, \tag{4}$$

where v_w and v_b are the group velocities of the electron in the well and the barrier, respectively. It should be noted that Eq. (2) is similar to the resonant behavior of light in the optical Fabry-Perot resonator.

C. Quantum wells with tunnel barriers at heterointerfaces

By analogy to the optical resonator, the resonant effect is expected to be dictated by the quality value of the QW resonator which is determined by the reflectivity of the interface mirror. The magnitude of the resonant effect is described as

$$\frac{\left|\frac{\Psi_w}{\Psi_b}\right|^2_{\text{resonance}}}{\left|\frac{\Psi_w}{\Psi_b}\right|^2_{\text{off-resonance}}}=\frac{\frac{v_b}{v_w}\frac{1+R}{1-R}}{\frac{v_b}{v_w}\frac{1-R}{1+R}}=\left[\frac{1+R}{1-R}\right]^2. \tag{5}$$

In a conventional QW structure, R is determined by v_w and v_b as shown in Eq. (3), and, therefore, by the depth of the potential well. In order to enhance the reflectivity R, we proposed a QW structure with tunnel barriers at QW interfaces.[18] The insertion of tunnel barriers at QW interfaces increases the reflectivity R of the interface mirror, corresponding to "high-reflectance coating" of the QW resonator in analogy to the optical resonator. In Fig. 1(a) the schematic picture of the resonant electron capture in QW's with tunnel barriers is shown, and the solid curves represent the behavior of the square amplitude of the electron wave function. In a QW with tunnel barriers under the resonant condition, the electron accumulates in the well, and consequently the electron position probability density in the well becomes much larger than that in the barrier. This is because the residence time of the electron in the well is significantly enhanced due to the high reflectivity of the electron at the QW in-

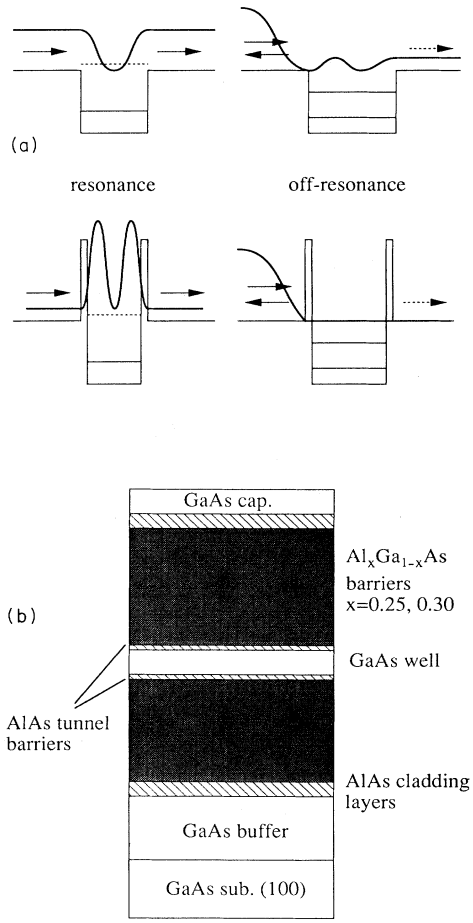

FIG. 1. (a) Schematics of the resonant electron capture in simple QW's and QW's with tunnel barriers. Solid lines represent the square amplitude of the wave function of the incoming electron from the left-side barrier. (b) Sample structures of $Al_xGa_{1-x}As/GaAs$ QW's with AlAs tunnel barriers. The width of the GaAs well layer is graded across the wafer surface.

terface with the tunnel barrier. In contrast, under the off-resonant condition, the electron is much less likely to enter the well than in the case of simple QW's under the off-resonant condition. Thus the resonant effect is expected to be enhanced in a QW with tunnel barriers. We can describe the resonant effect and the resonant conditions in a QW with tunnel barriers in the same way as the case of the simple QW as follows:

$$\left|\frac{\psi_w}{\psi_b}\right|^2 = \frac{|t_{wb}|^2\left[1+R+2\sqrt{R}\,\frac{\sin(2k_wL_z-\theta)+\sin\theta}{2k_wL_z}\right]}{(1-R)^2+4R\sin^2(k_wL_z-\theta)}, \quad (6)$$

where θ is the phase shift (delay) when the electron in the well is reflected back at the interface mirror with tunnel barriers. R, t_{wb}, and θ are given as

$$R=\left|\frac{v_{tb}(v_w-v_b)\cos k_{tb}L_{tb}-i(v_wv_b-v_{tb}^2)\sin k_{tb}L_{tb}}{v_{tb}(v_w+v_b)\cos k_{tb}L_{tb}-i(v_wv_b+v_{tb}^2)\sin k_{tb}L_{tb}}\right|^2, \quad (7)$$

$$t_{wb}=\frac{2v_bv_{tb}}{v_{tb}(v_w+v_b)\cos k_{tb}L_{tb}-i(v_wv_b+v_{tb}^2)\sin k_{tb}L_{tb}}, \quad (8)$$

$$\theta=\tan^{-1}\left\{\frac{-v_{tb}^2+v_wv_b}{v_{tb}(v_w-v_b)}\tan(k_{tb}L_{tb})\right\}+\tan^{-1}\left\{\frac{-v_{tb}^2-v_wv_b}{v_{tb}(v_w+v_b)}\tan(k_{tb}L_{tb})\right\}, \quad (9)$$

where L_{tb} is the width of tunnel barrier, and k_{tb} and v_{tb} are the imaginary wave number and the group velocity of the tunneling electron in the tunnel barrier, respectively. From Eq. (6), the resonant condition in the QW with tunnel barriers is obtained as

$$k_wL_z=(n-1)\pi+\theta \quad (n=1,2,3,\ldots). \quad (10)$$

It may be worth mentioning that a QW structure with tunnel barriers has another merit in experimentally observing the resonant carrier capture. We have already pointed out in Sec. I that one of the difficulties in observing the resonant carrier capture in QW's results from the fast capture time of carriers in QW's. It is expected that the carrier capture time is enlarged by the insertion of the tunnel barriers. The resonant effect in such a long-time scale is expected to be observed without being smoothed out by other energy relaxation processes.

III. EXPERIMENT

A. Sample preparation

$Al_xGa_{1-x}As$/AlAs/GaAs QW structures were grown by molecular-beam epitaxy (MBE) on semi-insulating GaAs(100) substrates. The MBE system is VG Semicon 80H with a background pressure of $\sim 10^{-10}$ Torr. We used solid sources of Ga (7N grade), Al (5N grade), and As (7N grade). The substrate temperature during the growth was usually kept at 580 °C. The growth rate and composition ratio of $Al_xGa_{1-x}As$ were determined by x-ray diffraction. A typical growth rate of GaAs was about 0.7 μ/h.

The schematic picture of the sample is shown in Fig. 1(b). The structure is composed of $Al_xGa_{1-x}As$ ($x=0.25$ and 0.3)/GaAs SQW with AlAs tunnel barriers. AlAs tunnel layers with various thickness ($L_{tb}=0$, 2.8 (1 ML), 10 and 20 Å) are inserted at the top and bottom QW interfaces. The whole QW structure is embedded between AlAs cladding layers to prevent carriers from overflowing out of the system into surface recombination centers. The width of the $Al_1Ga_{1-x}As$ barrier is chosen to be 750 Å, so that the electron in the $Al_xGa_{1-x}As$ barrier can establish coherent wave functions without any coherence-breaking scattering. In order to investigate the L_z dependence, we follow a special growth procedure. The sample was rotated during the growth of $Al_xGa_{1-x}As$ and AlAs layers and GaAs buffer layers in order to give a homogeneous layer thickness and composition ratio of $Al_xGa_{1-x}As$. In contrast, we intentionally stopped the substrate rotation during the growth of GaAs well layers. The rotation interruption led to a graded well width over the substrate due to spatial inhomogeneity of the Ga beam flux. The gradient of Lz, $\Delta Lz/Lz$, was typically 2.5% per 1 mm across the sample surface. The sample was typically 3–5 cm long. This method allowed us to systematically examine the L_z dependence of the carrier capture by the PL mapping technique with other parameters such as AlAs tunnel barrier widths and the barrier height of $Al_xGa_{1-x}As$ layers kept almost fixed. This technique also eliminates possible run-to-run fluctuation in the sample quality.

B. Photoluminescence measurements

We evaluated the carrier capture efficiency into QW's by means of PL measurements with an excitation source of a continuous-wave (cw) Ar^+ laser (514.5 nm) at temperatures of 22–200 K. The excitation power was 0.1–10 mW (typically 1 mW corresponding to an excitation intensity 10 W/cm^2). PL spectra were measured with a combined system of 1-m monochromator, a photomultiplier, and a lock-in amplifier. The carrier capture efficiency was estimated from the intensity ratio of the PL from the QW (I_w) and the $Al_xGa_{1-x}As$ barrier (I_b). The barrier carrier can take two kinds of relaxation pro-

cesses: radiative recombination in the barrier and capture into QW's. Therefore, we can evaluate the carrier capture process in terms of its competition with radiative recombination in the barrier. Typical PL spectra in QW's with 20-Å tunnel barriers are shown in the inset of Fig. 2. The PL peak from the $Al_xGa_{1-x}As$ barrier is clearly observed. This is because the tunnel barriers at QW interfaces reduce the carrier capture, resulting in a slow capture time. Even in the case of QW's with thinner tunnel barriers or no tunnel barriers, we could also observe the barrier PL, though it was weak. On the other hand, the barrier PL was not observed in samples without AlAs cladding layers. This indicates that AlAs cladding layers helped in preventing the carrier nonradiative decay via surface recombination. A clear observation of the barrier PL facilitates evaluation of I_w/I_b, enabling one to examine the L_z dependence of I_w/I_b by PL mapping over the sample and to study the dependence of the carrier capture efficiency on L_z.

We measured the carrier capture time in QW structures by means of time-resolved PL. The excitation source was a cavity-dumped pulse dye laser (Rhodamin6G) pumped by a mode-locked Ar^+-ion laser. The excitation wavelength was chosen to be 572 nm above the $Al_xGa_{1-x}As$ barrier band gap. The pulse duration was about 10 psec and the repetition rate was 4 MHz. The excitation density typically used was estimated to be 5×10^{10} cm^{-2}. Time-integrated PL spectra were taken with a cooled microchannel plate photomultiplier in the photon-counting mode. Time-resolved PL was measured by means of time-correlated single-photon counting. The detection wavelength was set at PL peaks. The system response time was evaluated to be 60–100 psec. The carrier capture time was determined by analyzing the temporal profile of the PL from the $Al_xGa_{1-x}As$ barriers.

IV. CARRIER CAPTURE EFFICIENCY

A. Well-width dependence of the carrier capture efficiency

Figure 2 shows the L_z dependence (50–130 Å) of I_w/I_b in the $Al_xGa_{1-x}As$ ($x=0.30$)/AlAs/GaAs QW with 20-Å tunnel barriers at 77 K. It is clearly seen that the carrier capture efficiency strongly depends on L_z and exhibits two sharp peaks. It was found from the calculation of the QW electronic states that the peak positions correspond to the well width when the highest bound states of QW's just line up with the $Al_xGa_{1-x}As$ barrier band edge. That is, the left-side peak at $L_z=67$ Å and the right-side peak at $L_z=107$ Å correspond to the resonances of the second ($n=2$) and the third ($n=3$) QW levels of electrons, respectively. Hence the peaks are identified as the resonant electron capture. The electron-capture efficiency is shown to be drastically increased due to the resonant electron capture, which is due to the enlarged resonant effect by the insertion of AlAs tunnel barriers. Although the resonant hole capture is also predicted,[5] however, no significant peaks corresponding to hole resonance are seen in this figure. This is probably because the coherent length of the heavy hole is smaller than that of the electron. Therefore, the classical capture process might dominate the hole capture and smooth out the quantum-mechanical capture process.

B. Tunnel-barrier-width dependence of the resonant electron capture

Figure 3 shows the L_z dependence of the carrier capture efficiency in $Al_xGa_{1-x}As$ ($x=0.25$)/AlAs/GaAs QW's with various L_{tb}'s. The resonance observed is ascribed to the resonant electron capture of the second ($n=2$) QW level. It is clearly seen that the resonant well width (L_{res}) increases with increasing L_{tb}. To explain the experimental results of L_{res}, we calculated L_{res} as a

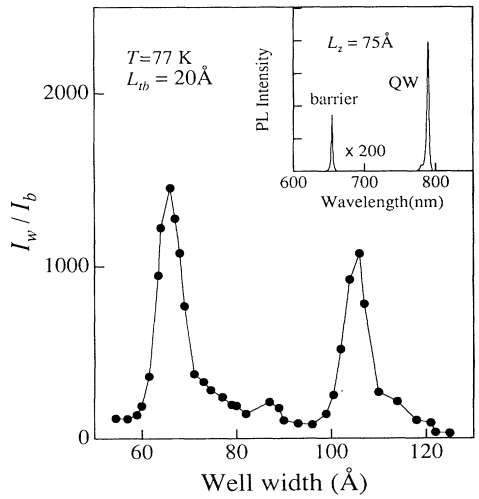

FIG. 2. Well-width dependence of the carrier capture efficiency in QW's with 20-Å tunnel barriers at 77 K. An oscillation due to the resonant electron capture ($n=2$ and 3) is clearly observed. The inset shows typical PL spectra.

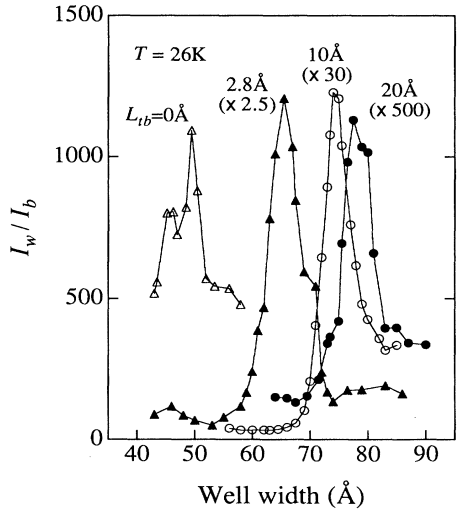

FIG. 3. Tunnel barrier width dependence (0, 2.8, 10, and 20 Å) of the resonant electron capture ($n=2$). Even 2.8 Å (1 ML) tunnel barriers drastically enhance the resonant effect.

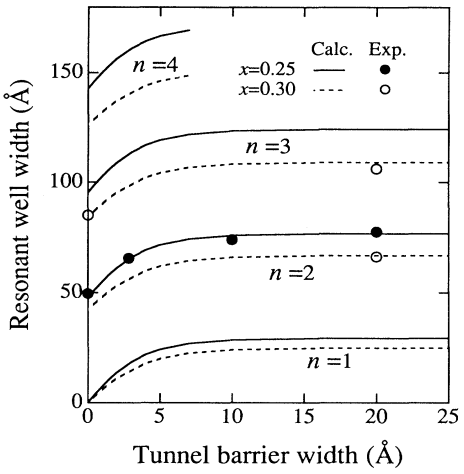

FIG. 4. The experimental and calculated resonant well width vs the width of the AlAs tunnel barriers. The calculation is based on the effective-mass approximation.

function of L_{tb} according to Eq. (10), as shown in Fig. 4. The parameters used in the calculation based on the effective-mass approximation are listed in Table I. The conduction-band nonparabolicity in the GaAs well layer was taken into account. This is because the resonant condition is a strong function of the wave number of electrons which have large kinetic energies in the well. The kinetic energy is nearly equal to the conduction-band offset (ΔE_c), 203 meV, for the $Al_{0.25}Ga_{0.75}As$ barrier, and 243 meV for the $Al_{0.3}Ga_{0.7}As$ barrier. Heiblum *et al.*[34] also pointed out the significance of the band nonparabolicity on the energy of QW virtual bound states in the study of ballistic electron transport.

It can be seen that the calculated results of L_{res} agree well with the experimental results including the case of 1-ML tunnel barriers. It is striking that the effective-mass approximation is applicable even to the case of 1-ML (2.8 Å) AlAs tunnel barriers. In the $Al_xGa_{1-x}As$ barrier, Al atoms are supposed to be randomly located at each site of Ga and Al atoms. Although 1 ML AlAs layers attached to such an alloy much have an adverse effect on the fluctuation of its width, it is surprising that they significantly work as tunnel barriers as described within the framework of the effective-mass approximation. Neu *et al.*[35] have also reported that the increased confinement energy by the insertion of 1–2 ML AlAs layers at $Al_xGa_{1-x}As/GaAs$ QW interfaces can be explained in terms of the effective-mass approximation. The L_{tb} dependence of L_{res} can be qualitatively interpreted as follows. For the simple QW ($L_{tb}=0$), the phase delay θ of reflected electrons at the $Al_xGa_{1-x}As/GaAs$ "interface mirror" is zero, and L_{res} is determined only by k_w, while the insertion of tunnel barriers produces the phase delay θ depending on L_{tb}, and consequently L_{res} is increased. In the latter case, both $Al_xGa_{1-x}As$ barriers and AlAs tunnel barriers make up the mirror of the QW resonator. With increasing L_{tb}, L_{res} shows a saturation behavior since the phase shift θ is dictated mainly by the GaAs/AlAs interface, and the $Al_xGa_{1-x}As$ barrier plays no large part as a mirror. It is also seen that L_{res} is smaller for the higher $Al_xGa_{1-x}As$ barrier. This is easily understood by considering that the energy matching of the QW levels with the $Al_xGa_{1-x}As$ barrier band edge occurs at smaller well widths for higher barriers.

C. Resonant feature and its temperature dependence

The resonant feature strongly depends on L_{tb}, since the resonant effect is dominated by the quantum-mechanical reflection at the QW interfaces. In order to compare clearly the resonant feature of various L_{tb}'s, we introduce a parameter called the "resonant enhancement factor" as $(I_w/I_b)_r/(I_w/I_b)_o$, which is the resonant I_w/I_b normalized by the off-resonant I_w/I_b.

In Fig. 5, the temperature dependence of the resonant enhancement factor for various L_{tb}'s is shown. Although the resonant enhancement factor strongly depends on temperature, it can be seen that it tends to increase with increasing L_{tb}. The resonant enhancement factors 69 for 20 Å tunnel barriers (60 K), 75 for 10 Å (43 K), 24 for 2.8 Å (26 K), and 6 for no tunnel barriers (22 K) were obtained at each maximum. It may be important to point out that "energy filtering effect" does not appear to have a serious effect. The resonant effect is enhanced by the increase of the reflectivity of the interface mirror. However, the resonant energy window for incident electrons tends to be narrower at the same time. The energy spectrum of the incident electrons is not monochromatic, but rather distributed due to thermal population and/or to

TABLE I. Parameters used in the calculation. Band-offset ratio between the conduction and valence bands $\Delta E_c/\Delta E_v=65/35$ (Refs. 31–33).

	GaAs	$Al_xGa_{1-x}As(0<x<0.45)$	AlAs
Eg^{Γ} (eV)	$1.519-5.405\times10^{-4}\ T^2/(204+T)$	$Eg^{\Gamma}(GaAs)+1.247x$	3.018
$m_e^{\Gamma}(m_0)$	$m_e^{\Gamma}=\hbar^2\left[\frac{d^2E}{dk^2}\right]^{-1}$		
	$E(k)\cong\frac{\hbar^2k^2}{2m_{e0}}+\alpha k^4$	$0.067+0.083x$	0.15
	$(m_{e0}=0.067m_0)$		
	$(\alpha=-2370\ \text{eV Å})$ (Ref. 30)		

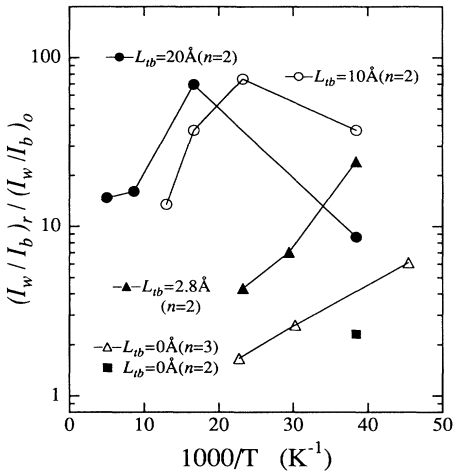

FIG. 5. Temperature dependence of the resonant enhancement factor with various L_{tb}'s. The resonant enhancement factor is defined as $(I_w/I_b)_r/(I_w/I_b)_o$, which is the resonant I_w/I_b normalized by the off-resonant I_w/I_b.

compositional inhomogeneity of the $Al_xGa_{1-x}As$ alloy barriers. As a result, when the resonant energy width (ΔE) is much smaller than this energy distribution, the resonant effect will be smoothed out. ΔE is equivalent to the energy width of the virtual bound state and can be estimated by

$$\Delta E = \frac{\sqrt{2}\hbar k_w}{m_e L_z} \sin^{-1}\left[\frac{1-R}{\sqrt{2(1+R^2)}}\right] . \quad (11)$$

By using Eq. (11), ΔE is estimated to be 3×10^{-2}, 1, and 15 meV for 20-, 10-, and 2.8-Å tunnel barriers, respectively. Meanwhile, the peak width of the $Al_xGa_{1-x}As$ barrier PL, which should reflect the energy distribution of electrons, was 4 meV (26 K) and 23 meV (200 K). According to this estimation, it is expected that the energy filtering effect should be significant in the case of 20-Å and 10-Å tunnel barriers. On the contrary, the experimental result displays a sharp resonance. There may be two possible explanations for this discrepancy. The first is the presence of the outer AlAs cladding layers. The trial frequency of the entrance to the QW could be increased, since the barrier electron can move back and forth between the AlAs cladding layer and the QW interface many times. The electron once reflected back off-resonantly at the QW interface can return and try again to enter the well. Consequently, the electron has several chances to enter the well resonantly by redistributing, while traveling in the barriers. The second reason is that ΔE probably can be larger than that calculated by Eq. (11). ΔE in Eq. (11) corresponds to the energy width of the virtual bound state and therefore is given by the inverse of the lifetime. The lifetime of the virtual bound state is defined as the time required for the electron to escape from the well into the barrier. However, the virtual bound state can obviously make another contribution to the lifetime in the relaxation process into the QW bound state via LO-phonon scattering. This time is of the order of picoseconds or subpicoseconds,[15,16] and the corresponding ΔE would amount to a few meV, resulting in reduction of the energy filtering effect.

It is noteworthy that the resonant enhancement factors obtained in this work are much larger than the peak-to-valley ratios (PVR's) that have been reported in conventional double-barrier resonant-tunneling diodes; e.g., 3.5 (at 300 K) (Ref. 36) and 13 (at 77 K) (Ref. 37) in $Al_xGa_{1-x}As$/GaAs resonant-tunneling diodes, and 3.2 (at 300 K) and 14 (at 77 K) (Ref. 38) in GaAs/AlAs/$In_xGa_{1-x}As$ resonant-tunneling diodes. The PVR is the ratio of the electric current between the resonant and off-resonant tunneling, and can be considered to be equivalent to the resonant enhancement factor in our measurements. The reason why the larger resonant enhancement factor was observed in PL measurements has not yet been clarified.

It is also seen Fig. 5 that the resonant enhancement factor is suppressed at low temperatures in the case of 10-Å and 20-Å tunnel barriers. The suppression of the resonance may be due to electron localization at low temperatures. In the case of thick tunnel barriers, the electron capture is slow, and consequently the electron in the barrier is likely to be localized at the local potential minima; that is, binding centers such as impurities and/or alloy disorder-induced band-gap fluctuations in the $Al_xGa_{1-x}As$ barrier. Such localized electrons cannot contribute to the resonant effect, and therefore the resonant effect of mobile electrons may be obscured. With increasing temperature, the resonant enhancement factor is seen to decrease, and in the case of no or thin tunnel barriers it starts to decrease at much lower temperatures. To show this behavior clearly, the temperature dependence of the resonant peak width is shown in Fig. 6. It can be seen that the width increases rapidly with temperature in the case of no and 2.8-Å tunnel barriers. In contrast, the resonant peak width is almost unchanged with temperature in the case of 20-Å tunnel barriers. The resonant peak width may have several origins. First of all,

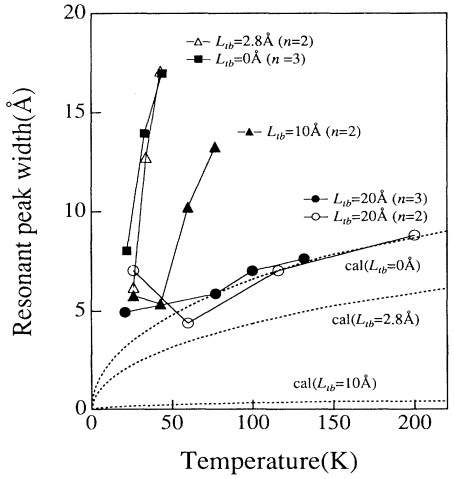

FIG. 6. Temperature dependence of the resonant peak width of various L_{tb}'s. Dotted lines represent the intrinsic peak width calculated by Eq. (12).

the resonant peak should have an intrinsic peak width, which reflects the quality factor of the QW resonator. The quality factor is determined by the reflectivity at the QW interface. In our model, the full width at half maximum of the resonant peak is a function of the reflectivity at the QW interface:

$$\Delta L_z = \frac{2}{k_w} \sin^{-1} \left[\frac{1-R}{\sqrt{2(1+R)^2}} \right] . \quad (12)$$

Here, note that R is a function of thermal energy of the incoming electron $E = -\frac{1}{2}kT$. The temperature dependence of the intrinsic ΔL_z is shown as dotted lines in Fig. 6. In the case of a QW with thick tunnel barriers, the calculated ΔL_z is very small and almost unchanged with temperature. This is because the thermal energy E is much smaller than the barrier height of AlAs, and, consequently, the reflectivity R hardly depends on E. The experiment is much larger and has an offset. The offset can be attributed to the inhomogeneous broadening due to L_z fluctuation in the sample. The sample grown has some L_z fluctuation due to interface roughness. The L_z fluctuation estimated from the peak width of the QW PL was about 2 Å, which is still smaller than the experiment. Probably the L_z fluctuation in the excited area where the carrier capture takes place is larger because the exciton in QW's emits a photon after it relaxes down to the wider well within the fluctuation, resulting in the Stokes shift well known in $Al_xGa_{1-x}As$/GaAs QW's. The resonant peak may be also broadened due to the energy distribution of the incident electron. However, the effect is very small because the energy distribution of 5 meV corresponds to ΔL_z less than 1 Å. In a QW with no or thin tunnel barriers, the experimental ΔL_z is much larger than the intrinsic ΔL_z, and increases drastically with increasing temperature. The strong dependence of ΔL_z on temperature might indicate that ΔL_z is determined by phonon scattering, which will break the electron wave coherence. The different temperature dependence might suggest that the electron-phonon-scattering mechanism is operating differently in the QW with no tunnel barriers and the QW with tunnel barriers.

V. CARRIER CAPTURE TIME

A. Well-width dependence of the decay time of $Al_xGa_{1-x}As$ barrier PL

In Fig. 7, the typical temporal profiles of $Al_xGa_{1-x}As$ barrier PL in the QW structures with 20-Å tunnel barriers are shown for three different L_z of 72, 81, and 85 Å. It is clearly observed that the decay behavior significantly depends on L_z. For a 81 Å QW, the PL decay is much faster than that of the other QW's. To clarify the L_z dependence of the decay time for the barrier PL, temporal profiles are analyzed by the simple three-level model. In this model, the photoexcited carriers relax down to the barrier-band edge with a time constant τ_r, and then decay with a time constant τ_d into QW's. Simple rate equations for such a process yield the temporal profile of the barrier PL to be

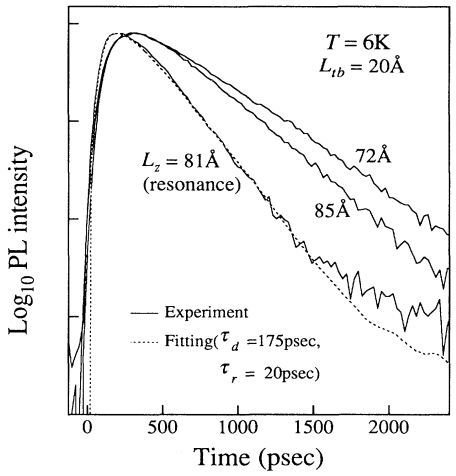

FIG. 7. Temporal profiles of $Al_{0.25}Ga_{0.75}As$ barrier PL in QW's with 20-Å tunnel barriers for $L_z = 72$, 81, and 85 Å. The dotted line is a fitted result by the three-level model.

$$I_b(t) = \frac{I_0(e^{-t/\tau_r} - e^{-t/\tau_d})}{\tau_r - \tau_d} . \quad (13)$$

Here I_0 is a constant. The convolution of this model profile and the system response is fitted to the experimental data. The fitted result is shown as a dotted line in Fig. 7 in the case of a 81-Å QW, and good agreement is obtained. The time resolution of this method is about 25 psec, which is limited by the resolution of the time-to-amplitude converter. τ_r was estimated to be 20–40 psec, and no dependence on L_z was obtained.

In Fig. 8, the L_z dependence of the decay time τ_d of the $Al_xGa_{1-x}As$ barrier PL is shown for the case of 20-Å tunnel barriers at 6 K. It is seen that the decay time

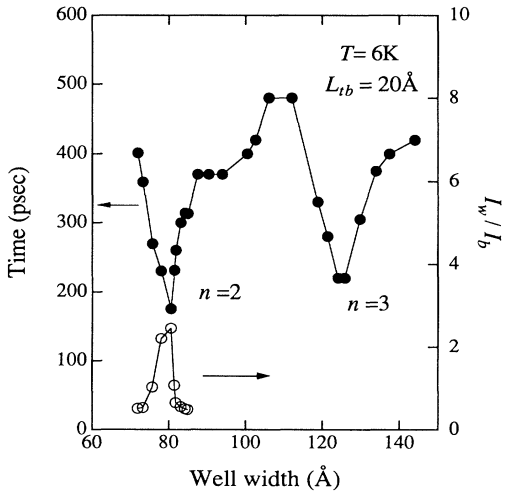

FIG. 8. The decay time of the $Al_{0.25}Ga_{0.75}As$ barrier PL vs the well width in QW's with 20-Å tunnel barriers. Dips due to the resonant electron capture ($n = 2$ and 3) are observed. Open circles represent the carrier capture efficiency I_w/I_b evaluated by time-integrated PL measurements.

shows strong oscillations between 175 and 480 psec with L_z. The oscillation can be ascribed to the resonant electron capture which appears periodically, since the well widths where the dips are observed coincide well with the resonant conditions described before. The left-side dip at 81 Å corresponds to the resonant electron capture of the second ($n=2$) QW level, and the right side to the third ($n=3$) QW level. The resonant electron-capture time was estimated to be 175 and 220 psec for $n=2$ and 3, respectively. It is seen in the figure that the dip in the decay time correctly corresponds to the resonant peak in carrier capture efficiency I_w/I_b evaluated by time-integrated PL measurements. It is also seen that the shapes of both curves are quite similar when one of them is plotted upside down, showing that the oscillation in decay time is due to the resonant electron capture. The decay time of the barrier PL is supposed to be affected by bipolar capture times for electrons and holes, and is dominated by the faster capture time. Hence the present observation may indicate that the electron-capture time is faster than that of holes, because the oscillating capture time due to the resonant electron capture was observed. This seems reasonable because the hole capture through tunnel barriers is expected to be slow due to its large effective mass. It should be added that these values were found to depend slightly on the excited carrier density in the range between 5×10^9 and 5×10^{10} cm^{-2}.

The successful observation of the resonant electron capture in the decay time measurements may result from the slow capture time in the presence of the AlAs tunnel barriers. For a simple QW without tunnel barriers, the capture time is of the order of a few picoseconds. The oscillation in such a fast time scale is easily washed out by other relaxation processes, and may be hard to observe even with subpicosecond techniques. In the present experiment, the decay time of the barrier PL for a simple QW could not be measured, because it was much faster than the time resolution of the experiment.

B. Tunnel-barrier-width dependence

Figure 9 shows the tunnel-barrier-width ($L_{\rm tb}$) dependence of the resonant feature for $n=2$ resonance. In the case of 20 and 10-Å tunnel barriers, the resonant electron capture is clearly observed, and capture times of 175 psec (20 Å) and 43 psec (10 Å) were obtained. The resonant well width is quite reasonable compared to the resonant condition calculated by the effective-mass approximation. In the case of 2.8-Å tunnel barriers, the resonant decay time is less than our time resolution, and the dip is not observed, while off-resonant capture time around 50 psec is obtained as seen in the figure.

In order to justify whether these values are reasonable as capture times or not, the resonant electron-capture time was roughly calculated based on the semiclassical model. The electron in the $Al_xGa_{1-x}As$ barrier periodically moves between the AlAs tunnel barrier at the QW interface and the AlAs cladding layer. When the electron encounters the QW under the resonant condition, the electron can tunnel through AlAs tunnel barriers into a virtual bound state in the well. It is assumed that the

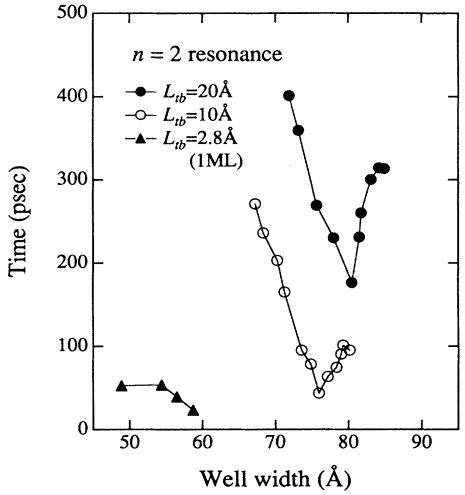

FIG. 9. Tunnel barrier width dependence of the $n=2$ resonant electron capture at 6 K.

electron, once inside the virtual bound state, is likely to relax to the bound state and be captured into QW's before escaping to the opposite $Al_xGa_{1-x}As$ barrier. We define the averaged time for the electron to enter the well as tunneling time as

$$\frac{1}{\tau_{\rm tun}}=f_t T_{\rm qw} \ . \tag{14}$$

Here $\tau_{\rm tun}$ represents the tunneling time and f_t corresponds to the frequency of the periodic motion of electrons in the $Al_xGa_{1-x}As$ barrier,

$$f_t=\frac{v_b}{2L_b} \ , \tag{15}$$

where v_b is the group velocity of the barrier electron, and L_b is the thickness of the $Al_xGa_{1-x}As$ barrier. Note that $T_{\rm qw}$ is the transmissivity of electrons through the QW resonator as given in Eq. (6). This is in contrast to the conventional calculation of tunneling time, in which the transmissivity of electrons through a single tunnel barrier is used. In such a conventional calculation, no resonant effect is considered. In order to deal with the resonant effect, the transmissivity through the whole QW structure should be used. In addition, the energy distribution of the incoming electron is considered, since the energy filtering effect is significant in QW's with tunnel barriers due to the high reflectivity at the QW interface. The tunneling time averaged over the energy distribution of the incoming electrons is calculated by

$$\overline{\tau_{\rm tun}}=\int_0^\infty \tau_{\rm tun}(E)f(E)dE \ , \tag{16}$$

where $\overline{\tau}_{\rm tun}$ represents the average capture time, and $f(E)$ is the energy distribution function of the incoming electron, a product of Maxwell-Boltzman distribution and the three-dimensional density of states. The calculated results are 1.4 nsec for 20-Å tunnel barriers and 16 psec for 10-Å tunnel barriers. The calculated time for 20-Å tunnel barriers is too large to explain the experimental result, which may be attributed to the overestimation of the

energy filtering effect. That is, the energy width may be much larger than the calculated energy width 0.03 meV, since the virtual bound state has a lifetime corresponding to the relaxation into the QW bound state via LO-phonon scattering. This time is of the order of picoseconds or subpicoseconds, and the energy width should be of the order of a few meV. Recently, Morris *et al.*[21] reported a resonant electron-capture time of 2 psec in similar structures with $Al_{0.5}Ga_{0.5}As$ tunnel barriers, which is shorter than the capture time of 20 psec estimated from our model. By taking into account LO-phonon scattering and impurity scattering, they obtained a better agreement with experiments. The quantitative estimation in our experiments remains a subject for future work.

C. Temporal profile of QW luminescence

The carrier dynamics in QW's are expected to be more complicated than those in the barrier, since various relaxation processes such as exciton formation, and relaxation of ($K \neq 0$) excitons into the ($K = 0$) excitons are important in QW's. Nevertheless, the capture time may affect the temporal profile of QW PL. When the captured electrons and holes form into excitons and the exciton radiatively recombines in QW's, it is expected that the decay time of QW PL reflects the exciton radiative recombination time, while the rise time corresponds to the slower capture time between electrons and holes. This is in contrast to the barrier PL, for which the decay time is dictated by the faster capture between electrons and holes. As discussed previously, the hole capture is thought to be much slower than that of the electron in the QW with tunnel barriers when the resonant electron capture occurs. Then the hole capture dominates the rise time of QW PL, and the resonant electron capture is supposed to have little influence on the time evolution of QW PL.

The decay time of the QW PL is shown as a function of L_z in Fig. 10. The decay time of the barrier PL in QW's with 20-Å tunnel barriers is also shown as a reference. In the case of 20-Å tunnel barriers, surprisingly, it is seen that the decay time is dependent on L_z, and that the fastest decay time is obtained in the resonant QW. It is also seen that both decay times of the QW and the barrier PL show similar resonant behaviors. The present result leads to the following speculations: (1) The decay time of QW PL is dominated by the carrier capture time, not by the exciton radiative recombination time. (2) The hole capture time is comparable to the electron-capture time. The first one may be possible if the exciton lifetime is faster than the capture time. As seen in Fig. 10, the decay time of QW PL tends to be faster with decreasing L_{tb}. Moreover, it is seen that the decay time becomes constant versus L_z at the bottom of the dip in QW's with 10-Å tunnel barriers, and that it is comparable to that of the no-tunnel barrier sample. These results suggest that the minimum decay time is around 150 psec, corresponding to the exciton lifetime in our samples. For thick tunnel barriers, the carrier capture time is longer than this time and is supposed to govern the decay time of QW PL, not the rise time. The hole capture is not an easy problem. There have been several reports contradicting the bipolar model of carrier capture or tunneling where the electron and the hole move independently of each other. Jackson *et al.*[39] investigated the tunneling time required for carriers to escape from the lowest quasibound state in QW's of GaAs/AlAs/GaAs/AlAs/GaAs double-barrier structures using PL excitation correlation spectroscopy. They observed a single tunneling time close to the tunneling time of electrons, and no signals of the hole tunneling were detected. They pointed out that the "charge buildup" effect is a possible explanation for the result. Due to the slower tunneling time for heavy holes than for the electron, QW's are likely to become negatively charged, resulting in band bending in such a way that it attracts holes toward QW's. Then the tunneling time of holes is increased. The charge buildup tends to continue until the tunneling times of electrons and holes become comparable. Blom *et al.*[23] also took into account the charge buildup effect to explain experimental results for resonant electron capture in $Al_xGa_{1-x}As/GaAs$ single QW's. In their interpretation, it is assumed that electron-capture and hole capture times are comparable due to the charge buildup effect; that is to say, "ambipolar capture." The present results of the decay time in QW's may indicate that the charge buildup effect also occurs. When resonant electron capture takes place, QW's are very likely to charge negatively, and the resultant band bending attracts holes, leading to a decrease of the hole capture time and then a decrease of the decay time of QW PL. This is a possible explanation for why QW PL decay time decreased under resonant electron capture.

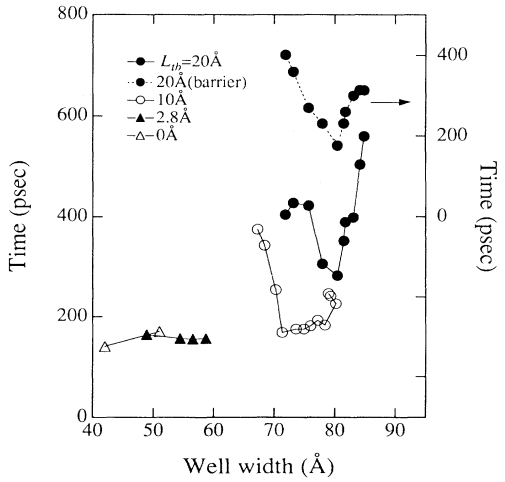

FIG. 10. Tunnel barrier width dependence of the decay time of QW PL. The decay time of the barrier PL is also reproduced as a reference in QW's with 20-Å tunnel barriers. The decay time of the QW PL shows a similar resonant dip.

VI. CONCLUSION

Resonant electron capture has been investigated systematically in terms of both capture efficiency and capture time in $Al_xGa_{1-x}As/AlAs/GaAs$ QW structures. The enhanced capture efficiency due to resonant electron capture has been observed clearly by cw PL measurements. It has also been revealed that the resonant effect

is drastically enhanced by the insertion of AlAs tunnel barriers at QW heterointerfaces. The resonant enhancement factors, 69 for 20 Å tunnel barriers (60 K), 75 for 10 Å (43 K), 24 for 2.8 Å (26 K), and six for no tunnel barriers (22 K), were obtained at each maximum. It has been found that the well width dependence of the resonance can be well described within the framework of the effective-mass approximation considering the conduction-band nonparabolicity. The time-resolved PL measurement clarified that the carrier capture time oscillatory changes due to the resonant electron capture between 175 and 480 and 43 and 270 psec for samples with 20-Å and 10-Å tunnel barriers, respectively. It has been shown that the resonant electron-capture time is reasonably explained by the modified semiclassical model. The ambipolar capture of the carriers due to the charge build-up effect has been suggested to be responsible for the temporal decay of the QW PL.

ACKNOWLEDGMENTS

We would like to thank Professor K. Onabe, Professor E. Hanamura, Professor M. Gonokami, Professor N. Ogasawara, Professor T. Osada, and Professor Y. Katayama for valuable suggestions. We wish to express our sincere thanks to Dr. K. Muraki for useful discussions and for their support on the time-resolved PL measurements. Thanks also to S. Ohtake for his technical support. This work is supported by a Grant-in-Aid from the Ministry of Education, Science, and Culture, Japan.

*Present address: NTT LSI Laboratories, 3-1, Morinosato Wakamiya, Atsugi, Kanagawa 243-01, Japan.

†Present address: Department of Electrical and Information Engineering, Yamagata University, Yonezawa-shi, Yamagata 992, Japan.

‡Present address: Department of Pure and Applied Sciences, The University of Tokyo, 3-8-1 Komaba, Meguro-ku, Tokyo 153, Japan.

[1]H. Shichijo, R. M. Kolbas, N. Holonyak, Jr., R. D. Dupuis, and P. D. Dapkus, Solid State Commun. **27**, 1029 (1978).

[2]R. D. Dupuis, P. D. Dapkus, R. M. Kolobas, N. Holonyak, Jr., and H. Shichijo, Appl. Phys. Lett. **33**, 596 (1978).

[3]J. Y. Tang, K. Hess, N. Holonyak, Jr., J. J. Coleman, and P. D. Dapkus, J. Appl. Phys. **53**, 6043 (1982).

[4]S. V. Kozyrev and Y. Ya. Shik, Fiz. Tekh. Poloprovodu. **19**, 1667 (1985) [Sov. Phys. Semicond. **19**, 1024 (1985)].

[5]J. A. Brum and G. Bastard, Phys. Rev. B **33**, 1420 (1986).

[6]G. Bastard, Phys. Rev. B **30**, 3547 (1984).

[7]G. Bastard, U. O. Ziemelis, C. Delalande, and M. Voos, Solid State Commun. **49**, 671 (1984).

[8]M. Babiker, M. P. Chamberlain, A. Ghosal, and B. K. Ridley, Surf. Sci. **196**, 422 (1988).

[9]B. Deveaud, J. Shah, T. C. Damen, and W. T. Tsang, Appl. Phys. Lett. **52**, 1886 (1988).

[10]J. Feldmann, G. Peter, E. O. Göbel, K. Leo, H.-J. Polland, K. Ploog, K. Fujiwara, and T. Nakayama, Appl. Phys. Lett. **51**, 226 (1987).

[11]D. J. Westland, D. Mihailovic, J. F. Ryan, and M. D. Scott, Appl. Phys. Lett. **51**, 590 (1987).

[12]H.-J. Polland, K. Leo, K. Rother, K. Ploog, J. Feldmann, G. Peter, E. O. Gobel, K. Fujiwara, T. Nakayama, and Y. Ohta, Phys. Rev. B **38**, 7635 (1988).

[13]B. Deveaud, F. Clerot, A. Regreny, K. Fujiwara, K. Mitsunaga, and J. Ohta, Appl. Phys. Lett. **55**, 2646 (1989).

[14]D. Y. Oberli, J. Shah, J. L. Jewell, T. C. Damen, and N. Chand, Appl. Phys. Lett. **54**, 1028 (1989).

[15]K. T. Tsen and H. Morkoç, Phys. Rev. B **38**, 5615 (1988).

[16]R. Ferreria and G. Bastard, Phys. Rev. B **40**, 1074 (1989).

[17]T. C. Damen, J. Shah, D. Y. Oberli, D. S. Chemla, J. E. Cunningham, and J. M. Kuo, Phys. Rev. B **42**, 7434 (1990).

[18]A. Fujiwara, S. Fukatsu, Y. Shiraki, and R. Ito, Surf. Sci. **263**, 642 (1992).

[19]A. Fujiwara, S. Fukatsu, Y. Shiraki, and R. Ito, in *International Workshop on Quantum Effect Physics, Electronics and Applications, Luxor, 1992,* edited by K. Ismail, IOP Conf. Proc. No. 127 (Institute of Physics and Physical Society, London, 1992), Chap. 5, p. 195.

[20]A. Fujiwara, S. Fukatsu, Y. Shiraki, and R. Ito, in *20th International Symposium on GaAs and Related Compounds, Freiburg, 1993,* IOP Conf. Proc. No. 136 (Institute of Physics and Physical Society, London, 1994), Chap. 4, p. 245.

[21]D. Morris, B. Deveaud, A. Regreny, and P. Auvray, Phys. Rev. B **47**, 6819 (1993).

[22]M. R. X. Barros, P. C. Becker, D. Morris, B. Deveaud, A. Regreny, and F. Beisser, Phys. Rev. B **47**, 10 951 (1993).

[23]P. W. Blom, C. Smit, J. E. M. Haverkort, and J. H. Wolter, Phys. Rev. B **47**, 2072 (1993).

[24]T. Mishima, J. Kasai, M. Morioka, Y. Sawada, Y. Murayama, Y. Katayama, and Y. Shiraki, in *12th International Symposium on GaAs and Related Compounds, Karuizawa, 1985,* edited by M. Fujimoto, IOP Conf. Proc. No. 79 (Institute of Physics and Physical Society, London, 1986), Chap. 8, p. 445.

[25]T. Mishima, J. Kasai, M. Morioka, Y. Sawada, Y. Katayama, Y. Shiraki, and Y. Murayama, Surf. Sci. **174**, 307 (1986).

[26]N. Ogasawara, A. Fujiwara, N. Ohgushi, S. Fukatsu, Y. Shiraki, Y. Katayama, and R. Ito, Phys. Rev. B **42**, 9562 (1990).

[27]A. Fujiwara, S. Fukatsu, Y. Shiraki, and R. Ito (unpublished).

[28]D. Bohm, *Quantum Theory* (Prentice-Hall, New York, 1951).

[29]A. Messiah, *Quantum Mechanics* (North-Holland, Amsterdam, 1970).

[30]T. Ruf and M. Cardona, Phys. Rev. B **41**, 10 747 (1990).

[31]H. Kroemer, W. Y. Chien, J. S. Harris, Jr., and D. D. Edwall, Appl. Phys. Lett. **36**, 295 (1980).

[32]R. C. Miller, A. C. Gossard, D. A. Kleinman, and O. Munteanu, Phys. Rev. B **29**, 3740 (1984).

[33]D. Arnold, A. Ketterson, T. Henderson, J. Klem, and H. Morkoç, J. Appl. Phys. **57**, 2880 (1985).

[34]M. Heiblum, M. V. Fishetti, W. P. Dumke, D. J. Frank, I. M. Anderson, C. M. Knoedler, and L. Osterling, Phys. Rev. Lett. **58**, 816 (1987).

[35]G. Neu, Y. Chen, C. Deparis, and J. Massies, Appl. Phys. Lett. **58**, 2111 (1991).

[36]W. D. Goodhue, T. C. L. G. Sollner, H. Q. Lee, E. R. Brown, and B. A. Vojak, Appl. Phys. Lett. **49**, 1086 (1986).

[37]V. J. Goldman, D. C. Tsui, and E. Cunningham, Phys. Rev. Lett. **58**, 1256 (1987).

[38]R. Kapre, A. Madhukar, K. Kaviani, S. Guha, and K. C. Rajkumar, Appl. Phys. Lett. **56**, 922 (1990).

[39]M. K. Jackson, M. B. Johnson, D. H. Chow, and T. C. McGill, Appl. Phys. Lett. **54**, 552 (1989).

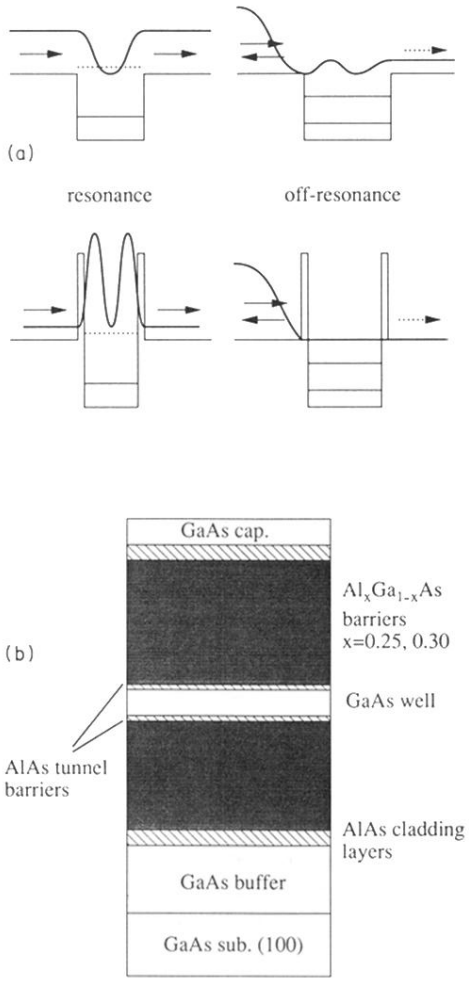

FIG. 1. (a) Schematics of the resonant electron capture in simple QW's and QW's with tunnel barriers. Solid lines represent the square amplitude of the wave function of the incoming electron from the left-side barrier. (b) Sample structures of $Al_xGa_{1-x}As/GaAs$ QW's with AlAs tunnel barriers. The width of the GaAs well layer is graded across the wafer surface.